

# APPLICATION OF ICA TO MEG NOISE REDUCTION

*Masaki KAWAKATSU*

Tokyo Denki University, Chiba, JAPAN

## ABSTRACT

It is important to reduce noise in MEG measurement, since the signal to noise ratio is smaller than 1.0, even in magnetically shielded room environment. ICA is a powerful tool for noise reduction in MEG measurements.

We have applied ICA to various MEG data. By using ICA, we can remove the cardiac field, power line noise and other noises from MEG data. Also, we succeeded in extracting auditory evoked field from non-averaged MEG data. ICA produces many independent components in MEG, but usually their classification into relevant and irrelevant components depends largely on subjective judgment. We propose a criterion for judging which of the obtained independent components comprise MEG components, and in particular the evoked response using the signal subspace obtained from the averaged response. This method often worked effectively to reconstruct single evoked responses based on the objective criterion. Although there still remain many problems. The application of ICA to MEG data, should further be studied because 'noninvasive' study of the brain activities intrinsically implies 'blind' separation of activities.

## 1. INTRODUCTION

In 1970, D. Cohen reported the first recording of magnetoencephalography (MEG) using SQUID (Superconductive Quantum Interference Device). Until now, MEG has proved to be a useful tool in clinical applications in many aspects of neurological and psychological brain research.

MEG is a very weak magnetic field which is produced within the brain. The field is smaller than  $1/10^8$  of the earth magnetic field. The only kind of detector that has the required sensitivity for MEG measurement is the SQUID magnetometer. However, there are many sources of magnetic noise which interfere with MEG measurements.

The noise sources are, for example, power lines, electric motors, trains, cars, or portable phones. According to a report, the noise of a train was 400 nTp-p about 190 m away from the track. The noise of a car about 8 m away was 100 – 150 nTp-p. The mechanical vibrations can also be a cause of the noise. Nearby roads with traffic may be

one source of vibrations. The sensor has its intrinsic noise which is called 'sensor noise'. A typical dc-SQUID magnetometer noise is  $5 \text{ fT/Hz}^{1/2}$  at 10 Hz.

In the experiment, eye movement and blinks generate artifacts. These noises are 10 to 20 times larger than evoked signals. The heart also generates noise field which can be about 10 times the signal. (We would like to point out that the cardiac noise depends greatly on the shape and arrangement of the pickup coils.) In addition, artifacts may be caused by mechanical movement of the body with breathing. Furthermore, background brain activities also become a noise for evoked magnetic field measurement. The amplitude of the alpha band brain activities is about 10 times that of the evoked magnetic field. Sometimes these noises synchronize to the stimuli. In that case, they are difficult to remove by averaging. In the study of MEG, experimental tasks performed by the subjects are restricted by the averaging procedure. For example, the measurement of the olfactory response is difficult, because it is not possible to perform averaging over many epochs without adaptation of the subjects to the stimuli. Moreover, it is reported that the components remaining spontaneous activities after averaging affect the signal source estimation[1].

Significant reduction of noise by ICA or other methods would result in such improvements as the reduction of the cost of magnetically shielded room, and getting better evoked responses with less averaging. Furthermore, it may even be possible to measure single evoked responses without averaging and to see detailed structures in them which are averaged out in the conventional procedure due to their variation.

## 2. SOME NOISE REDUCTION METHODS

**Magnetically Shielded room:** The most ordinary method for noise reduction is to use a magnetically shield room. This room is enclosed with the layers of high ferromagnetic metal. Figure 1 shows the shielded room in our laboratory, which is enclosed in a capsule made of four layers of permalloy and one of aluminum. It attenuates external fields by 100 dB at 1 Hz.

**Gradiometer:** The sensor consists of two or more coils, taking the difference between the fields measured by the coils. This arrangement is insensitive to a homogeneous



Figure.1 A magnetically shielded room at Tokyo Denki University.

magnetic field and sensitive to nearby signal sources. Since brain magnetic fields are not homogeneous, gradiometers can reduce the noise from a long distance.

Reference sensor: Some MEG system has extra sensors only for noise measurement. Since these sensors are positioned far away from the subject's head, they detect distant noise sources. From noise sensor's output, one can compute some of the gradient field. Thus, it is equal to a virtual gradiometer. By devising noise sensors, it could realize 2 or 3 order gradiometer.

Filtering and averaging: Filtering is a simple way to reduce the wideband noise. The typical cut-off frequency in MEG measurements is 0.03 – 1.0 Hz for high pass filter, and 40 – 400 Hz for low pass filter. Averaging is also a simple way for measurement of evoked responses. By averaging, noises are canceled out, and the signal which is synchronized with the stimuli remains. However, it could not remove the noise which synchronized with stimuli.

### 3. SIGNAL SUB-SPACE PROJECTION (SSSP)

There are some noise reduction methods by software like PCA[2] and SSP (Signal Space Projection)[3]. The PCA method is based on the fact that the first component of PCA for non-averaged data is irrelevant to evoked fields. On the other hand, the SSP method removes a noise vector known *a priori*. (For example, power line, train or vibrations).

However, these two methods may drastically reduce the signal when the degree of orthogonality of noise and signal in the sensor space is insufficient, even if the S/N ratio is large. To overcome this difficulty, we propose the method of estimating the subspace spanned by the sensor outputs[4]. It is estimated from feature extraction of the lead-field vectors for uniformly distributed points in the head.

### 3.1. Method

The lattice points for calculating the lead field are positioned in the hemisphere that approximates the head. The radius of the hemisphere is 8 cm and the center is at  $x=y=z=0$ . The lattice points are placed at 1cm intervals. If the geometrical configuration of the head and sensor array of  $K$  sensors are given, we can calculate the lead field vector  $\mathbf{L}_{\{2(i-1)+j\}}$  for  $i=1,2,\dots,M$ ,  $j=1,2$ , where  $M$  is the number of the lattice points, by Sarvas's equation[5].  $\mathbf{L}_{\{2(i-1)+1\}}$  is the vector of which the  $k$ -th element represents the field measured by the  $k$ -th sensor when there is a current dipole of unit intensity in  $\theta$  direction at the  $i$ -th lattice point.

$\mathbf{L}_{\{2(i-1)+2\}}$  is defined in the same manner for the dipole in  $\varphi$  direction. We define the normalized lead field matrix to be  $\mathbf{L}=\{\mathbf{L}_1/|\mathbf{L}_1|, \mathbf{L}_2/|\mathbf{L}_2|, \dots, \mathbf{L}_{2M}/|\mathbf{L}_{2M}|\}$ . The lead field vectors in  $\mathbf{L}$  are normalized so that the dipoles in the deeper regions may not be neglected. (This may be a controversial point in this method.) We then apply PCA to the matrix  $\mathbf{L}\mathbf{L}^T$ , namely, we take the  $N$  eigenvectors  $\mathbf{e}_1, \dots, \mathbf{e}_N$  of  $\mathbf{L}\mathbf{L}^T$  corresponding to the first  $N$  eigenvalues from the largest one which, when summed, exceed 99.9 % of the sum of all the eigenvalues. The  $K \times N$  matrix  $\mathbf{S}_L$  is defined to be  $\mathbf{S}_L=\{\mathbf{e}_1, \dots, \mathbf{e}_N\}$ . The space spanned by  $\mathbf{e}_1, \dots, \mathbf{e}_N$  is a  $N$ -dimensional subspace in the signal space  $\mathbf{R}^K$  and we call it the signal subspace.  $N$  was usually 40-50 for  $K=195$  for the whole head MEG system[6] but varied according to the sensor type and sensor positions. Let  $\mathbf{b}$  be the  $K$  dimensional vector of the measured field. The filtered  $\mathbf{b}^*$  is obtained as the orthogonal projection of  $\mathbf{b}$  to the signal subspace:

$$\mathbf{b}^* = \mathbf{S}_L \mathbf{S}_L^T \mathbf{b} = \sum_{i=1}^N (\mathbf{b} \cdot \mathbf{e}_i) \mathbf{e}_i \quad (1)$$

This is considered as a linear system  $\mathbf{b}^* = \Gamma \mathbf{b}$  with  $N \times N$  matrix  $\Gamma = \mathbf{S}_L \mathbf{S}_L^T$ . Since it is the orthogonal projection to the signal subspace, those components of the measurement vector which are orthogonal to the subspace are filtered out as noise while those components considered as signal would not be changed.

### 3.2. Simulation

In order to examine its effectiveness, simulation study was carried out as follows. Our whole head MEG system had 65 detection sites, each site containing three gradiometers which were designed to measure the 3 dimensional vector field. We obtained by the Sarvas's equation the 195(=65×3) dimensional measurement vector  $\mathbf{b}(\mathbf{r})$  produced by a current dipole at position  $\mathbf{r}$ . The dipole was assumed to be positioned on the line  $y=0$  [m],  $z=0.01$  [m]

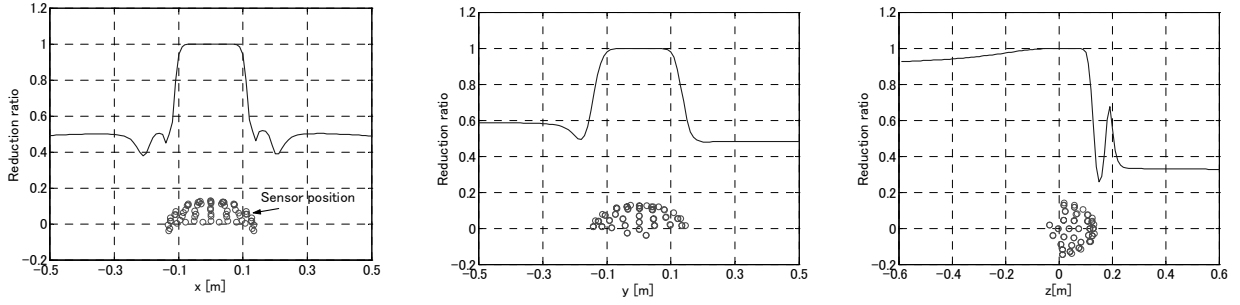


Figure 2 The filtering characteristic of the orthogonal projection to the signal subspace for the 195-ch vector measurement system. Each graph is the plot of the amplitude ratio where  $\mathbf{b}(\mathbf{r})$  is the measurement vector for the current dipole placed at  $\mathbf{r}$  and  $\Gamma \mathbf{b}(\mathbf{r})$  is the projection to the subspace (see text). The dipole was assumed to be on the line (a)  $y=0$  [m],  $z=0.01$  [m], (b)  $x=0$  [m],  $z=0.01$  [m], (c)  $x=0$  [m],  $y=0.01$  [m]. The small circles show SQUID sensor positions.

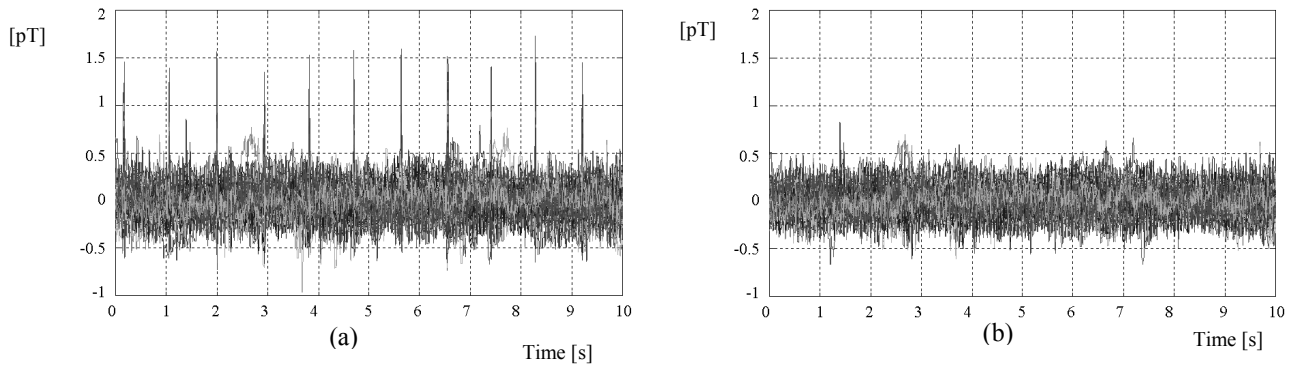


Figure 3 (a) The superimposed traces of non-averaged magnetic fields measured with repeated stimulus of tone bursts (see text). (b) The same data noise reduction by ICA. The cardiac activity has been removed.

and moved from  $x=-0.5$  to  $0.5$  [m]. The filter is characterized by the following amplitude reduction:

$$R(\mathbf{r}) = \|\Gamma \mathbf{b}(\mathbf{r})\| / \|\mathbf{b}(\mathbf{r})\| \quad (2)$$

where,  $\|\cdot\|$  is the  $L_2$  norm. It is seen in figure 2 that the method functions as an effective spatial filter in  $x$ - $y$  plane,  $R(\mathbf{r})$  is around 0.5 for  $\mathbf{r}$  outside the sphere and almost 1 for  $\mathbf{r}$  inside the sphere. Notice that the natural norm of  $\Gamma$  is 1. The filter however does not suppress the signal from  $z < -0.8$  [m], which is due to the configuration of the sensors.

### 3.3. Experiment

Auditory evoked field (AEF) measurement was made in our magnetically shielded room using our whole-head 195-channel SQUID MEG system for detecting vector fields. The signals from detector were filtered by analog bandpass filter (0.1-100 Hz) and notch filter at 50 Hz. The sampling frequency was 400Hz. The subjects were 3 right-handed male (22 - 30 years). The stimuli consisted of 1 kHz tone bursts (100 ms duration, 10 ms rising and falling time.) to the right ear. The inter stimulus interval

was 900 ms. The signals were further filtered by FIR digital filter with cut-off frequency of 45 Hz. The signal subspace method was applied to averaged AEF data obtained with stimuli repeated 10, 20 and 50 times. Noise reduction of 20 - 30 % was achieved in each case, which was not sufficient for AEF measurements but of some value for preprocessing.

## 4. NOISE REDUCTION BY ICA

### 4.1. Data acquisition

Auditory evoked magnetic fields were obtained from four normal subjects (22-30 years old, male) by the same procedure as described in section 3.3. The superimposed 195 channel non-averaged data are shown in Fig.3 (a).

### 4.2. Preprocessing

First, FIR low-pass filter with cut of frequency of 40 Hz was applied to the data and then the DC component was removed. We used FA (factor analysis) for dimension reduction from 195 to  $m$  which was determined such that the extracted factors explained for 70 % of the total vari-

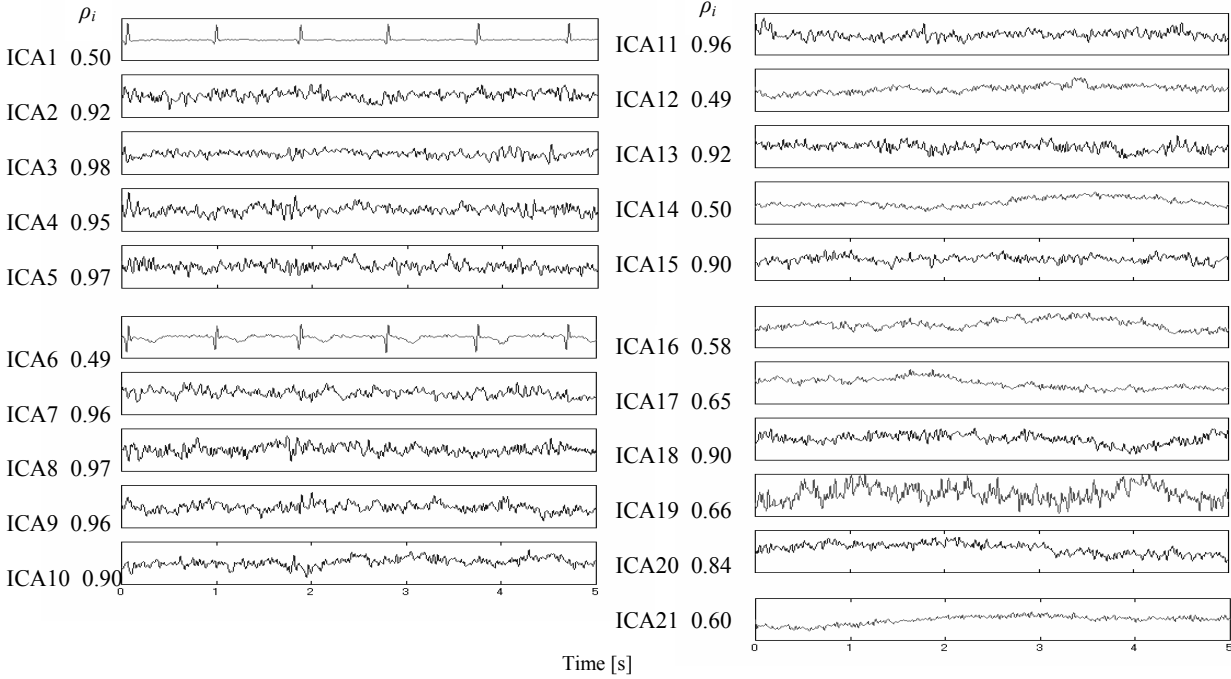


Figure 4: The independent components extracted from the MEG data measured with tone burst stimuli. The number to the left of each trace is the value of  $\rho_i$  measured with respect to the signal subspace (see text). Cardiac activity have been extracted (ICA1, ICA6), and found to have small values of  $\rho_i$  as expected. ICA14, 16 and 17 show small values of and thus were treated as noise; they may probably due to some drift in measurement system.

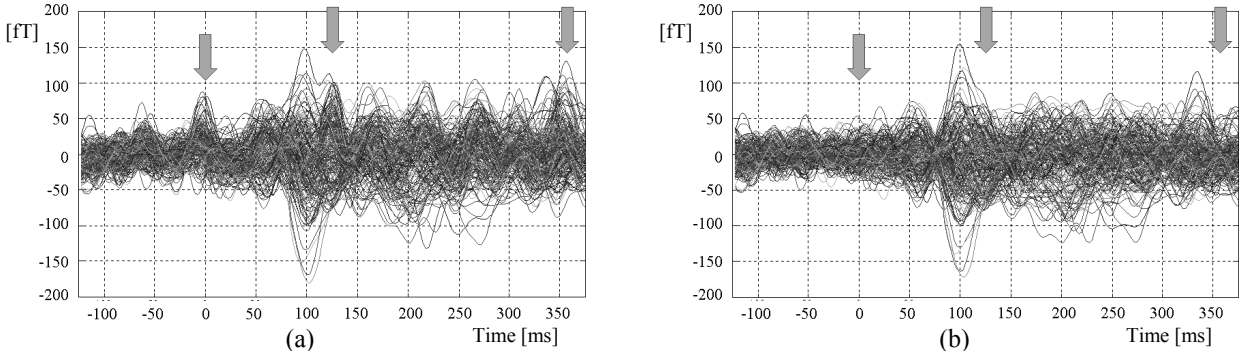


Figure 5 Superimposed traces of auditory evoked magnetic field obtained by averaging 30 epochs. (a): without and (b): with the proposed ICA noise reduction.

ance. The  $m$  ranged between 11 and 23 for the data we treated.

### 4.3. ICA

JADECOR (Joint Approximate Diagonalization Estimator based on Correlation function) algorithm[7,8] was applied to the data preprocessed by FA. One set of data consisted of 20000 sample points or 50 s in duration. Then we estimated the mixture matrix  $\hat{\mathbf{A}}$  and independent components

$$\hat{\mathbf{y}} = [\hat{\mathbf{y}}_1, \hat{\mathbf{y}}_2, \dots, \hat{\mathbf{y}}_m]. \quad (3)$$

### 4.4. The selection of the noise components

The independent components are to be distinguished the magnetic fields which caused by the brain activity from the other magnetic fields. We proposed a method using signal subspace method. The matrix  $\hat{\mathbf{W}} = [\hat{\mathbf{w}}_1, \hat{\mathbf{w}}_2, \dots, \hat{\mathbf{w}}_m]$  is pseudo inverse of  $\hat{\mathbf{A}}$ . The component  $\hat{\mathbf{y}}_i$  is selected as noise when corresponding  $\hat{\mathbf{w}}_i$  failed to satisfies the following inequality.

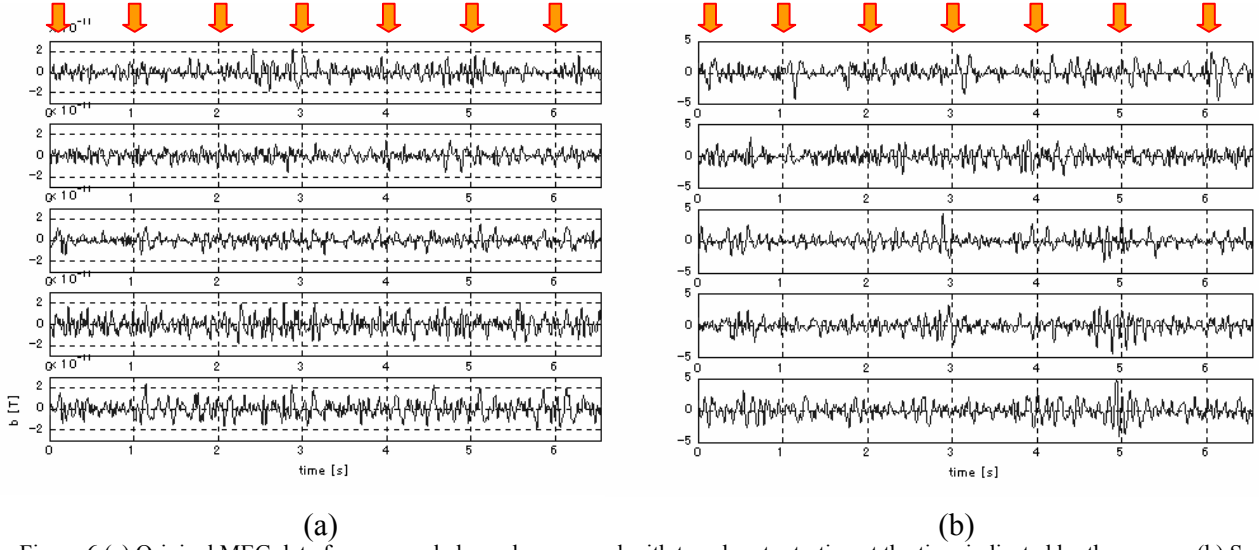


Figure.6 (a) Original MEG data from several channels measured with tone bursts starting at the time indicated by the arrows. (b) Some of the extracted independent components.

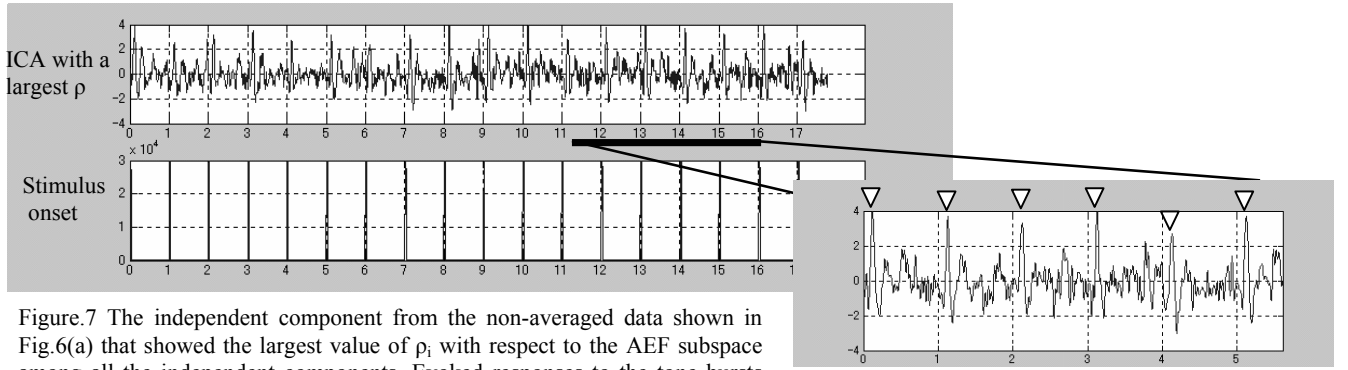


Figure.7 The independent component from the non-averaged data shown in Fig.6(a) that showed the largest value of  $\rho_i$  with respect to the AEF subspace among all the independent components. Evoked responses to the tone bursts are clearly seen as indicated by the triangles in the inset.

$$\rho_i = \frac{\|\hat{\mathbf{w}}_i^T \mathbf{S}_L\|}{\|\hat{\mathbf{w}}_i\|} \geq c \quad (4)$$

where  $\mathbf{S}_L$  is the matrix of the vectors spanning the signal subspace defined in section 3.1.  $0 < c < 1$  is a positive constant. We found  $c=0.7$  to be a good choice. The independent components classified as noise were used to reconstruct the ‘noise’ field for each component of the measurement vector. Then it was subtracted from the measured data.

#### 4.5. Results

Fig.3 (a) shows the superimposed traces of the fields measured by the 195 sensors on subject A. The cardiac field is clearly seen. The above mentioned method using FA and ICA extracted 21 independent components (Fig.4). ICA1 and ICA6 are apparently of the cardiac activity and ICA14, ICA16 and ICA17 probably come from some drift present in the measurement system. They are to be ex-

cluded as noise from the above criterion with  $c=0.7$ . The MEG traces after subtraction of the irrelevant components according to the criterion are shown in Fig.3 (b). The most apparent feature is that the cardiac activity present in (a) is no more seen. Fig. 5 shows the averaged responses of 30 epochs. Without the noise reduction procedure, the cardiac activity remains even after averaging (a) but vanished if the proposed procedure was applied before averaging (b). Due to the reduction of noise, the evoked response can be seen more clearly in (b).

### 5. EVOKED COMPONENT EXTRACTION

#### 5.1. Signal subspace for AEF

The method in the previous chapter using the signal subspace constructed from the lead fields removed those components considered to come from outside the brain quite successfully. However, in AEF measurement, the background spontaneous activities of the brain have also

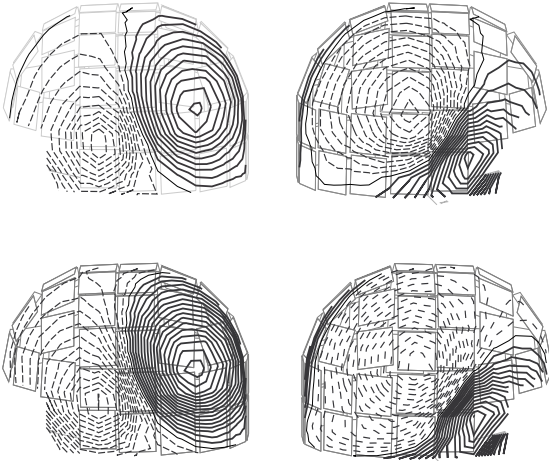


**Figure.8.** The Contour maps of the averaged AEF (top) and of the reconstructed ICA component (bottom). The left columns show the left hemisphere, and the right columns show the right hemisphere.

to be removed because they produce much larger fields than the AEF. To do this we proposed to use the following signal space estimated from the averaged data[4]. Let  $\mathbf{b}_{av}(t_i)$  be the  $K$ -dimensional averaged measurement vector at time  $t_i$  from the onset of the stimulus. Let the  $K \times K$  matrix:

$$\mathbf{C} = \sum_{i=1}^I \mathbf{b}_{av}(t_i) \mathbf{b}_{av}(t_i)^T$$

and use this as the covariance matrix for the standard PCA procedure.  $N$  eigenvectors were chosen so that the accumulated variance first exceeded 90 % of the total variance. These eigenvectors  $\{\mathbf{e}_i\}$  now form the basis of the signal subspace which we here call the AEF subspace.

## 5.2. Measurement and Result

Four normal male subjects (age; 21-31, right handed) participated in this study. The auditory evoked magnetic fields were measured in a magnetically shielded room using Neuromag 122-channel whole-cortex SQUID system. The signals were filtered (0.03 - 100 Hz) and sampled at 1024 Hz. We used the data over the span of the first 20000 sample points for analysis of non-averaged field. The auditory stimulus consisted of 1000 Hz tone bursts delivered to the right ear through a tube with  $\sim 1.0$  s intervals between. The template average response  $\mathbf{b}_{av}(t_i)$  was obtained by averaging the field measured for 60 epochs. The non-averaged field was processed by FA and ICA as in sections 4.2 and 4.3 and the dimension 122 of the data was reduced to  $m$  through this procedure such that about 80 % of the total variance was reproduced by the  $m$  components. The component  $\hat{\mathbf{y}}_i$  is selected as evoked components when corresponding  $\hat{\mathbf{w}}_i$  satisfies eq.(4).

Fig.6 (a) shows the data before processing and (b) shows the extracted components. Fig.7 shows the extracted independent component  $\mathbf{y}_i(t)$  with the largest  $\rho_i$  ( $=0.78$ ) among all the components. Peaks are clearly seen with a latency of  $\sim 0.1$ s after each onset of the tone burst. Furthermore, Fig.8 shows the similarity between the distribution of the averaged auditory evoked field and of the reconstructed signal ICA component. This indicates that the reconstructed field in Fig.7 actually represents the evoked field. For other three subjects also, we observed reconstructed fields and their distributions which were very likely to be evoked fields.

## 6. DISCUSSION

In the present paper we presented methods of noise reduction by using the signal subspace, and of noise reduction and AEF detection by ICA combined with FA. Noise reduction using the signal subspace alone was limited in its effectiveness but formed the basis for the component selection in ICA analysis. Noise reduction by ICA which proved effective for removing cardiac artifacts and some system noise was made possible by the signal subspace. For AEF detection, which was able in some cases to extract the evoked responses from non-averaged data, the signal subspace was replaced with 'AEF' subspace which was constructed from the averaged response. Thus ICA combined with FA and signal or AEF subspaces was shown to perform satisfactorily for noise reduction or AEF detection from non-averaged data when the original data were of good quality. However, some problems still remain in applying ICA to MEG data. For example, the results depended on the dimension  $m$  after ICA combined with FA, to considerable degree. If  $m$  was too large, ICA tended to divide a component which seemed to be a reasonable one response as a whole into several independent components which may not have physiological or psychological counterparts. Even if we determine  $m$  by a certain criterion like the proportion of the total variance explained for by the selected components, the value of  $m$  is influenced by such factors as the environmental noise, sensor type, background activity of the brain and by the experimental tasks assigned to the subject. Therefore, there is still much room for subjective choice of  $m$ . Also, our method of choosing certain independent components as irrelevant noise or as AEF using the subspaces has some arbitrariness in the choice of the value of  $c$  in eq. (4) which, however does not pose such a serious problem. A more basic problem may be that ICA assumes that the sources are statistically independent with each other while there are probably many sources of evoked fields with the brain. For example, the left and right auditory cortices produce evoked fields which are certainly strongly correlated. Moreover, in the somatosensory system for example, a stimulus first elicits evoked responses in S-I cortex

which then sends the information to S-II cortex. Therefore, S-I and S-II produce evoked responses which are correlated with a delay. The method we have employed may have difficulty in situations like these. Several methods have been proposed to deal with noisy data and data convoluted temporally as well as spatially. It will be important to develop ICA methods suitable for MEG measurement. It will also be an interesting and challenging problem to design a measurement system (sensor coils and their arrangement, etc.) optimal for the ICA procedure.

### Acknowledgements

The author thanks Dr. I. Nemoto, Dr. Y. Uchikawa and Dr. M. Kotani for helpful discussion. The author also thanks Mr. K. Watanabe, Mr. H. Ishibashi and Mr. A. Fujimoto for their help in experiments. This work is supported by the Ministry of Education, Culture, Sports, Science and Technology of Japan, and Futaba Electronics Memorial Foundation.

### References

- [1] K. Sekihara, F. Takeuchi, S. Kuriki, H. Koizumi, "Reduction of brain noise influence in evoked neuromagnetic source localization using noise spatial correlation", *Phys. Med. Biol.*, 39, 937-946, 1994.
- [2] K. Kobayashi, S. Kuriki, "Principal component elimination method for the improvement of S/N in evoked neuromagnetic field measurements", *IEEE trans. Biomed. Eng. & Comput.*, 35, 135-140, 1997
- [3] M. Uusitalo, R.J. Ilmoniemi, "Signal-Space Projection method for separating MEG or EEG into components.", *Med. Biol. Eng. Comp.* 35, pp. 135-140, (1997).
- [4] M. Kawakatsu, K. Kobayashi et. al., "A noise reduction using signal-subspace method", In J. Nenonen, R.J. Ilmoniemi, and T. Katila (Eds) *Biomag2000*, Helsinki University of Technology, 903-906, 2001.
- [5] J. Sarvas, "Basic mathematical and electro-magnetic concepts of the biomagnetic inverse problem", *Phys. Med., Biol.*, No.32, pp.11 – 22, 1987.
- [6] M. Kotani, Y. Uchikawa, M. Kawakatsu et.al., "A Whole-Head SQUID System For Detecting Vector Components", *Applied Superconductivity*, Vol. 5, Nos 7-12, 399-403, 1998
- [7] J.-F. Cardoso and A. Souloumiac, "Jacobi angles for simultaneous diagonalization", *SIAM J. Mat. Anal. Appl.*, Vol.17, No.1, 161-164, 1996.
- [8] L. Molgedey, H. G. Schuster, "Separation of mixture of independent signals using time delayed correlations", *Phys. Rev. Lett.* 72, 3634-3637, 1994